

**A.D. Thamir**

Department of Production  
Engineering and Metallurgy,  
University of Technology,  
Baghdad, Iraq.

**K.A. Sukkar**

Research Center of  
Nanotechnology and  
Advanced Materials,  
University of Technology,  
Baghdad, Iraq.  
[khalid\\_ajmee@yahoo.com](mailto:khalid_ajmee@yahoo.com)

**Ali A. Ati**

Research Center of  
Nanotechnology and  
Advanced Materials,  
University of Technology,  
Baghdad, Iraq.  
[aliphysics1@gmail.com](mailto:aliphysics1@gmail.com)

## Improve the Process of Enhancing Oil Recovery (EOR) by Applying Nanomagnetic Cobalt Ferrite Nanoparticles

***Abstract**-In this paper we reported nano-crystalline cobalt ferrite powders were synthesized using co-precipitation method at 600 °C, 700 °C and 800 °C. The structural, morphological and magnetic properties of the powders were investigated by x-ray diffraction (XRD), Fourier transform infrared (FTIR) spectroscopy, transmission electron microscopy (TEM) and vibrating sample magnetometer (VSM). Infrared spectral analysis data between 200 and 1000 cm<sup>-1</sup> defined the intrinsic cation vibrations of the characteristic spinel structure system. The saturation magnetization (M<sub>s</sub>) and coercivity (H<sub>c</sub>) of the CoFe<sub>2</sub>O<sub>4</sub> were found to be in the range of 94-33 emu/g, which is still in the range of hard ferrite. The observed variation in saturation magnetization, coercivity and remanence magnetization as a function of increasing the temperature and grain size of samples. From this point of view, nano-scale size of nanoparticles makes them efficient for using in borehole stability maintaining for enhancing oil and gas recovery efficiency improvement. The large value of magnetic pressure (-2.95699) are expected to be useful in oil recovery applications. It has also been found that the choice of nanoparticles for application in oil recovery depends on nature, magnetic and electric properties of the reservoir rock.*

***Keywords**-Chemical method; Magnetic nanoparticles; VSM; FT-IR; Oil recovery*

---

How to cite this article: A.D. Thamir, K.A. Sukkar and Ali A. Ati, "Improve the Process of Enhancing Oil Recovery (EOR) by Applying Nanomagnetic Cobalt Ferrite Nanoparticles," *Engineering and Technology Journal*, Vol. 35, No. 9, pp. 872-877, 2017.

---

### 1. Introduction

Recently, many researcher have reported in the study of several spinel-type ferrites particle by different synthesization techniques give potential application of nanosized magnetic materials in different technological areas [1]. This is due to ferrites nanoparticle prepared by various method of preparation, annealing temperature, and the doping concentration exhibit dissimilar structural properties. The selection of an appropriate process is essential in obtaining good quality ferrites [2]. Among the different spinel-type ferrites, cobalt-ferrites are the most magnetic materials for general use. Why choose cobalt instead of other ferrite material? It is because not like other soft ferrite such as Mn-Zn ferrite, Ni-Zn ferrite has lower resistivity and therefore it can prevent eddy current, which is another source of energy loss. Cobalt ferrite has a very high resistivity; it is suitable for frequency over 1 MHz and high temperature applications. Compound that contain cobalt are extensively used in the cores of RF transformer or electromagnetic cores and inductors in application such as switch-mode power supplies. Cobalt ferrites also known as ferromagnetic materials with a huge number of technological applications in telecommunications

and entertainment electronics. Hence, in this present studies intend to synthesize cobalt ferrite powders produced by co-precipitation method. This approach will allow us to directly determine, examine, understand and distinguish the morphological on the nanostructure out of all alternative method. Structural and magnetic properties of spinel ferrite nanocrystals are affected by their compositions and synthesis methods. In present research, a few method which have been reported previously for the preparation of cobalt ferrite nanocrystal such as sol gel method [3,4], and many else. Although some method give many advantage such as saving in time for making the sample and low cost but from the past research, the composition of respective substitution that come from different method gives many different result. In this research, we try to improve, development and selecting the excellent productions for oil recovery application according to various parameters such as nano scale, saturation magnetization, susceptibility and magnetic pressure of these nanoparticles.

## 2. Experimental

Chemical composition cobalt ferrite will be prepared using co-precipitation process using stoichiometric amount of  $\text{Co}(\text{CH}_3\text{COO})_2 \cdot 4\text{H}_2\text{O}$ ,  $\text{Fe}(\text{NO}_3)_3 \cdot 9\text{H}_2\text{O}$  (98.5%, Merck) and NaOH (99%, Merck) as a raw materials. In order to prepare the sample, the chemical were weighted by using analytical balance. Iron (III) nitrate solution were mixed together with cobalt acetate in de-ionized water with continuous stirring and heated under constant at 80 °C. After 2 hours, NaOH solution is added drop-wise at 70 °C to form precipitate. Then, the co-precipitate product are washed several times with de-ionized water until pH of filtered water reach about 7-8. The precipitate are filtered and dried overnight into the furnace at 150 °C to remove water content. Next step is the precipitate will go under heat treatment or often called as calcination for 8h prior to the measurement at different temperature, which are 600 °C, 700 °C and 800 °C. XRD, FT-IR, TEM and VSM are used for structural, morphological and magnetic properties.

## 3. Result and Discussion

The cobalt ferrite samples has been successfully prepared by using co-precipitation method. Ferrite samples obtained were in a powder and dark color form. The structural properties of cobalt ferrite nanoparticles is performed at room temperature by using a X-ray diffractometer (XRD, D8 Advanced) with Cu-K $\alpha$  radiations (1.54178 Å) at 40 Kv and 10 mA. Through this technique, it will give the information on average particle size, x-ray density, volume, crystallinity, and lattice parameter [5-8]. The x-ray diffraction pattern for  $\text{CoFe}_2\text{O}_4$  annealed at 600 °C, 700 °C and 800 °C are presented in Figure 1. For each ferrite samples, peaks are indexed to 311, 400, 422, 511 and 440 planes indicated the formation of crystalline single phase cubic spinel structure corresponding to those three temperature. Analysis of diffraction pattern showed that for the same composition that annealing with different temperature show that the peaks grew sharper as we increase the annealing temperature. Hence, it is indicate that an increase in the crystallize size related with temperature. The excellent structure

at 700 °C and 800 °C, show the best structure as because there is no extra peaks [9].

The broadening of the X-ray diffraction peaks for as prepared sample is related to the nanocrystalline partical size. The average particle sizes of ferrite nanocrystalline are determined from the XRD spectra using Debye-Scherrer's formula.

$$D = \frac{K\lambda}{\beta \cos\theta} \tag{1}$$

Where  $\lambda$  is the wavelength of the X-ray radiation,  $\beta$  is full width at half maximum (FWHM) of line broadening and K is a constant taken as 0.9, and  $\theta$  is the angle of diffraction.

The most intense peak (311) are used to estimate the average particle sizes of nanocrystallites where it show the crystallinity of the structure. The various of average particle size in correspond to those three annealing temperature are summarized in Table 1. It is observed that the average particle size of nanoparticles are estimated to be ~15 nm, ~21 nm, and ~24 nm when annealed at 600 °C, 700 °C and 800 °C, respectively.

Beside, each composition of cobalt ferrite indicating an increase in the crystallize size as we increase the annealing temperature.

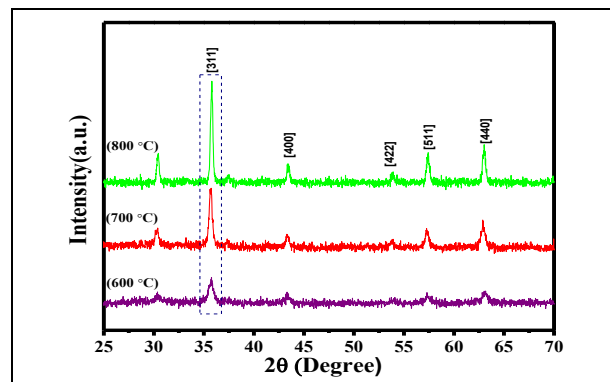


Figure 1: XRD Spectra of  $\text{CoFe}_2\text{O}_4$  annealed at (a) 600 °C, (b) 700 °C and (c) 800 °C.

Table 1: Data of average crystallize size of  $\text{CoFe}_2\text{O}_4$  annealed at 600 °C, 700 °C and 800 °C.

Composition	Crystallite size (nm)		
	600 °C	700 °C	800 °C
Temperature	600 °C	700 °C	800 °C
$\text{CoFe}_2\text{O}_4$	14.77 ± 0.0	20.89 ± 0.0	23.92 ± 0.1
	7	8	1

## VII. Footnotes

The lattice constant ' $a_{exp}$ ' for ferrite samples with different temperature was estimated using  $d$ -spacing of the diffracting planes using the Bragg's law [10].

$$n\lambda = 2d_{hkl}\sin\theta \quad (2)$$

where  $\lambda$  is the X-ray wavelength ( $\lambda = 0.154 \text{ \AA}$ ),  $d$  is the inter-planar spacing and  $2\theta$  is the measured diffraction angle of peak position. From the crystal structure which is in this case is a cubic for spinel, the lattice constant is calculated from this  $d$ -spacing by using following formula.

$$a_{exp} = \sqrt{d^2(h^2 + k^2 + l^2)} \quad (3)$$

Where (hkl) are Miller indices. Therefore by examining the diffraction angles of the peaks in each ferrite sample, the lattice constant can be calculated and compared with temperature. For each specimen, the lattice constant was averaged from strongest spinel cubic structure peaks which is (311). The calculated lattice parameter ' $a$ ' is seen to increase from  $8.351 \text{ \AA}$  to  $8.393 \text{ \AA}$  and  $8.428 \text{ \AA}$  at  $600 \text{ }^\circ\text{C}$ ,  $700 \text{ }^\circ\text{C}$  and  $800 \text{ }^\circ\text{C}$ , respectively, as reported in Table 2.

The X-ray density of all the samples was determined using the following relation:

$$d_x = \frac{ZM}{Na^3} \quad (4)$$

Where ' $Z$ ' is the number of molecules per unit cell ( $Z = 8$ ), ' $M$ ' is the molecular weight,  $a^3$  is volume and ' $N$ ' is the Avogadro's number. The density of x-ray calculated from the XRD pattern is summarized in Table 3. For temperature  $600 \text{ }^\circ\text{C}$ ,  $700 \text{ }^\circ\text{C}$ , and  $800 \text{ }^\circ\text{C}$ , it was seen from the table that the x-ray density decrease as the temperature increase. This is because from Eq. (4) indicated that x-ray density is depend on the lattice parameters and molecular weight of compositions. If the x-ray density is decrease, then the volume of nanoparticle must increase. In the following Table 4 show that the volume of cobalt ferrite of all the samples are increase with temperature increase.

**Table 2: Lattice parameter data for  $\text{CoFe}_2\text{O}_4$  annealed at  $600 \text{ }^\circ\text{C}$ ,  $700 \text{ }^\circ\text{C}$ , and  $800 \text{ }^\circ\text{C}$ .**

Composition	Lattice Parameter, a ( $\text{\AA}$ )		
	$600 \text{ }^\circ\text{C}$	$700 \text{ }^\circ\text{C}$	$800 \text{ }^\circ\text{C}$
$\text{CoFe}_2\text{O}_4$	8.351	8.393	8.428

**Table 3 X-ray density data of  $\text{CoFe}_2\text{O}_4$  annealed at  $600 \text{ }^\circ\text{C}$ ,  $700 \text{ }^\circ\text{C}$ , and  $800 \text{ }^\circ\text{C}$ .**

Composition	X-ray density ( $\text{g/cm}^3$ ),		
	$600 \text{ }^\circ\text{C}$	$700 \text{ }^\circ\text{C}$	$800 \text{ }^\circ\text{C}$
$\text{CoFe}_2\text{O}_4$	4.274	4.256	4.247

**Table 4 Cell volume of  $\text{CoFe}_2\text{O}_4$  annealed at  $600 \text{ }^\circ\text{C}$ ,  $700 \text{ }^\circ\text{C}$ , and  $800 \text{ }^\circ\text{C}$ .**

Composition	Cell volume ( $\text{\AA}^3$ )		
	$600 \text{ }^\circ\text{C}$	$700 \text{ }^\circ\text{C}$	$800 \text{ }^\circ\text{C}$
$\text{CoFe}_2\text{O}_4$	582.39	591.22	598.65

The room temperature FTIR spectra recorded in the wave-number range of  $250\text{-}1000 \text{ cm}^{-1}$  are shown in Figure 2. The result of the vibrational frequencies are summarized in Table 4. Ferrite can be described as continuously bonded atoms as they are bonded closely to all the nearest neighbors by Van der Waals interaction. In ferrite the metal ions occupy different sublattices which are tetrahedral (A-site) and octahedral (B-site). The FTIR spectra of cobalt spinel ferrite consisting of two absorption bands, which are  $\nu_1$  and  $\nu_2$ , confirm the presence of A (tetrahedral) and B (octahedral) sub-lattices.  $\nu_1$  is the vibrational frequency of the tetrahedral or called as A-site and  $\nu_2$  is the vibrational frequency of the octahedral or called as B-site. The higher absorption band  $\nu_1$  is due to the stretching vibration mode of metal-oxygen in the tetrahedral sites, while  $\nu_2$  is related to octahedral group complexes.

The morphology, size distribution and shape of the cobalt ferrite sample were examined using high-resolution transmission electron microscope (HR-TEM) and 3D-Image J software are shown in Figure 3. The irregular particle sizes of the ferrite specimen prepared at  $800 \text{ }^\circ\text{C}$  is in agreement with that obtained from x-ray diffraction. HR-TEM images confirm the formation of more or less spherical in shape and the particles size less than  $25 \text{ nm}$  with slight agglomeration because of exchange the interaction with the heat treatment or may be due to nano-scale of ferrite particles have a large surface area, which results to interfacial surface tension. Another reason of the agglomeration may be due to magneto-static interaction between the nanoparticles because of high reactivity of ferrite sample with the heat treatment process. Hysteresis loops obtained for cobalt ferrite samples prepared at  $600 \text{ }^\circ\text{C}$ ,  $700 \text{ }^\circ\text{C}$  and  $800 \text{ }^\circ\text{C}$  are displayed in Figure 4. Saturation magnetization of these samples are found lower than cobalt bulk ferrite [11]. The variation in magnetic susceptibility value ( $\chi$ ) of the ferrite samples with increasing the synthesised

temperature may be due to increases in samples ferrite size. For magnetic materials and the magnetic fields of moderate strength, and are co-linear.

$$\chi = M/H \tag{5}$$

These results are supported by the well-known tendency of variation in the saturation magnetic saturation in response to the increasing temperature.

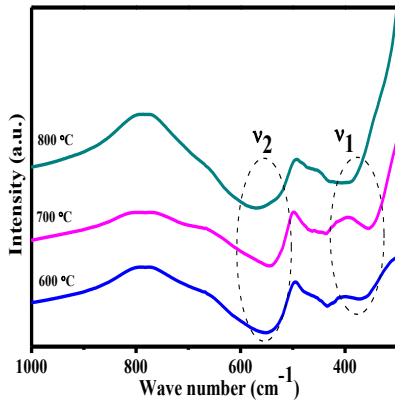


Figure 2: FTIR vibrational frequencies of CoFe<sub>2</sub>O<sub>4</sub> annealed at 600 °C, 700 °C, 800 °C.

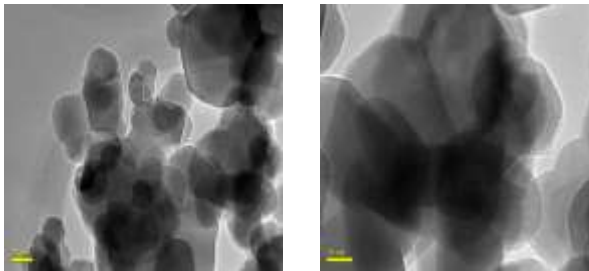


Figure 3: TEM image of the cobalt ferrite sample at 800 °C.

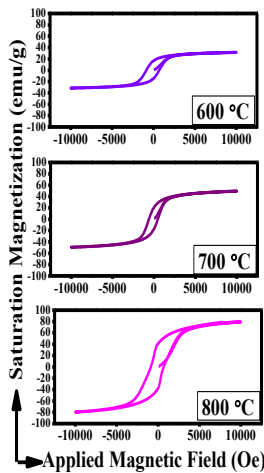


Figure 4. The room temperature M–H curves of CoFe<sub>2</sub>O<sub>4</sub> at different temperature.

After synthesized of magnetic nanoparticles by chemical process for enhanced oil recovery is applied to extract the residual oil from the reservoir. Different mechanisms like interfacial tension reduction and wettability alteration change are associated with recovery of trapped oil from reservoir. The interaction between two immiscible phases implies the interfacial energy. Attraction between the substrates causes lower interfacial energy, and repulsion forces result in higher energy surface. According to the Young-Laplace equation, the interface at equilibrium supports a pressure difference (so called capillary pressure ‘P<sub>c</sub>’), and thus defined as,

$$P_c = P \text{ (non-wetting phase) (NW)} - P \text{ (wetting phase) (W)} \tag{6}$$

The Young-Laplace equation states that this pressure difference is proportional to the interfacial tension,

$$P_c = \frac{2\gamma \cos\theta}{r} \tag{7}$$

Where ‘ $\gamma$ ’ Interfacial tension, ‘ $r$ ’ effective radius and ‘ $\theta$ ’ wetting angle (contact angle).

The wetting of surface and spreading of liquid are most influencing factors in oil recovery mechanism. It is very well known that surface active agents can alter wettability of rock surface and thereby changes the wettability condition to favorable of oil production. In general, wettability affects capillary pressure and relative permeability curves, which govern the oil recovery efficiency. Recently several studies show that nanoparticles have great impacts on wettability alteration mechanism and these nanoparticles are very effective in oil recovery. Nanoparticles are used in terms of nanofluids for changing wettability alteration. The magnetic nanoparticle structuring and magnetic phenomenon play an important role on structural disjoining pressures.

The magnetic stress tensor and the fact that the normal components of  $B$  and tangential component of  $H$  are continuous across the NW-W interface, the interface at equilibrium curves in order to satisfy a modified Young-Laplace equation as follows:

$$P_c - (P_s + P_m + P_n) - \sigma k = 0 \tag{8}$$

$$P_{NW} - P_W - (P_s + P_m + P_n) = \sigma k \tag{9}$$

$$\sigma(\gamma) = P_{NW} - P_W - (P_s + P_m + P_n) / k \tag{10}$$

$$P_m = \frac{1}{2} \mu_0 \chi H^2 \tag{11}$$

$$P_s = \frac{1}{2} \mu_0 \chi H^2 \frac{\rho_1 - \rho_2}{\rho_1} \tag{12}$$

$$P_n = \frac{1}{2} \mu_0 \chi^2 H^2 \tag{13}$$

where  $P_s$  is the Magnetostrictive pressure,  $P_m$  is a Fluid-magnetic pressure,  $P_n$  is Magnetic normal pressure, Vacuum permeability ( $\mu_0$ ) is  $4\pi \times 10^{-7}$ ,  $\rho_1$  is water density ( $1000 \text{ kg/m}^3$ ),  $\rho_2$  is oil density at  $100^\circ\text{C}$  ( $822.966 \text{ kg/m}^3$ ) and  $K$  is curvature of the interfaces. Magnetostrictive pressure having a negative effect, due to the external pressure would never be completely compensated by the internal pressure.

The variations in the magnetic susceptibility ' $\chi$ ' and pressures with increasing temperature are attributed to the cations distribution between both sites of cobalt ferrite samples [12] reported the magnetic properties of ferrite nanoparticles with varying compositions like Fe, Al to determine the magnetic responses of the various particles in the oil and gas industry. Two types of nanoparticles like nano- $\text{Fe}_3\text{O}_4$  and nano- $\text{AlFe}_2\text{O}_4$  were used for

experimental purpose. Different experimental techniques said that nano- $\text{Fe}_3\text{O}_4$  is the ideal nanoparticles and it shows highest magnetic susceptibility and permeability at  $27^\circ\text{C}$  and  $100^\circ\text{C}$  respectively. All parameters have nonlinear relationship with magnetic field, the increase or decrease value of the pressures dependence on the magnetic susceptibility. The assignments for the susceptibility and pressure are summarized in Table 5 and Table 6. When the total magnetic pressure is negative that will guide us to two options, the first one is water-wet rock, means the effect of capillary pressure increase and the other one oil-wet rock, here the effect of capillary pressure decrease [13].

**Table 5: The room temperature magnetic parameters**

Composition	B(G)	H (A/m)	$M_s$	$M_r$	$\chi$
$\text{CoFe}_2\text{O}_4$	726.15	57814.46	76.508	15.747	0.013
$\text{CoFe}_2\text{O}_4$	143.15	11397.28	33.478	9.158	0.029
$\text{CoFe}_2\text{O}_4$	143.81	11449.83	94.996	20.142	0.082

**Table 6: Magnetostrictive pressure, fluid-magnetic pressure, magnetic normal pressure and total magnetic pressure for magnetic nanoparticles pressure parameters for each composition at room temperature**

Composites	$P_m$ (Pa)	$P_s$ (Pa)	$P_n$ (Pa)	$P_m+P_s+P_n$ (Pa)
$\text{CoFe}_2\text{O}_4$ ( $600^\circ\text{C}$ )	27.288	-154.12	0.3547	-126.4773
$\text{CoFe}_2\text{O}_4$ ( $700^\circ\text{C}$ )	2.365	13.3615	0.0686	-10.9279
$\text{CoFe}_2\text{O}_4$ ( $800^\circ\text{C}$ )	6.75106	-38.129	0.5535	-30.8244

#### 4. Conclusion

Cobalt ferrite nanopowders have been successfully synthesized by co-precipitation method. The structural and magnetic properties characterization nanoparticles have been investigated using XRD, FT-IR and VSM. Co-substitutions have great effects on the structural as well as magnetic properties of the prepared samples. The infrared spectra show two prominent bands corresponding to the spinel ferrite phase. Magnetization was found to exist in the range of 33.47-94.99 emu/g and coercivity lies in the range of 98.08-726.15 Oe. From the literature, it was found that nano scale size of nanoparticles makes them efficient for using in borehole stability maintaining for enhancing oil and gas recovery efficiency improvement. The large value of magnetic pressure (-2.95699) are expected to be useful in oil recovery applications.

#### Acknowledgments

The authors would like to thank the University of Technology/Center of Nanotechnology and Advanced Materials, Universiti Teknologi Malaysia for the funding of the project and Ibnu Sina Institute for Fundamental Science Studies and Physics Department of UTP for the technical supports.

#### References

- [1] A. Costa, V. Silva, D.R. Cornejo, M. Morelli, R. Kiminami, L. Gama, Magnetic and structural properties of  $\text{NiFe}_2\text{O}_4$  ferrite nanopowder doped with  $\text{Zn}^{2+}$ , Journal of Magnetism and Magnetic Materials, 320 (2008) e370-e372.
- [2] R. Peelamedu, C. Grimes, D. Agrawal, R. Roy, P. Yadoji, Ultralow dielectric constant nickel-zinc ferrites using microwave sintering, Journal of materials research, 18 (2003) 2292-2295.
- [3] L. Avazpour, M.R. Toroghinejad, H. Shokrollahi, Enhanced magneto-optical Kerr effect in rare earth

- substituted nanostructured cobalt ferrite thin film prepared by sol-gel method, *Applied Surface Science*, 387 (2016) 869-874.
- [4] L. Yao, Y. Xi, G. Xi, Y. Feng, Synthesis of cobalt ferrite with enhanced magnetostriction properties by the sol-gel-hydrothermal route using spent Li-ion battery, *Journal of Alloys and Compounds*, 680 (2016) 73-79.
- [5] A. Amirabadizadeh, Z. Salighe, R. Sarhaddi, Z. Lotfollahi, Synthesis of ferrofluids based on cobalt ferrite nanoparticles: Influence of reaction time on structural, morphological and magnetic properties, *Journal of Magnetism and Magnetic Materials*, 434 (2017) 78-85.
- [6] K.K. Kefeni, B.B. Mamba, T.A.M. Msagati, Magnetite and cobalt ferrite nanoparticles used as seeds for acid mine drainage treatment, *Journal of Hazardous Materials*, 333 (2017) 308-318.
- [7] M. Ristic, S. Krehula, M. Reissner, M. Jean, B. Hannover, S. Musić, Synthesis and properties of precipitated cobalt ferrite nanoparticles, *Journal of Molecular Structure*, 1140 (2017) 32-38.
- [8] T. Sodaee, A. Ghasemi, R. Shoja Razavi, Cation distribution and microwave absorptive behavior of gadolinium substituted cobalt ferrite ceramics, *Journal of Alloys and Compounds*, 706 (2017) 133-146.
- [9] A.A. Ati, Z. Othaman, A. Samavati, Influence of cobalt on structural and magnetic properties of nickel ferrite nanoparticles, *Journal of Molecular Structure*, 1052 (2013) 177-182.
- [10] B.T. Naughton, *Magnetic nanoparticles for power electronics*, (2006).
- [11] N. Deraz, A. Alarifi, Microstructure and magnetic studies of zinc ferrite nano-particles, *Int J Electrochem Sci*, 7 (2012) 6501-6511.
- [12] C. Avendano, S.S. Lee, G. Escalera, V. Colvin, Magnetic Characterization of Nanoparticles Designed for Use As Contrast Agents for Downhole Measurements, in: *SPE International Oilfield Nanotechnology Conference and Exhibition*, Society of Petroleum Engineers, 2012.
- [13] M. Prodanovic, S. Ryoo, A.R. Rahmani, R.V. Kuranov, C. Kotsmar, T.E. Milner, K.P. Johnston, S.L. Bryant, C. Huh, Effects of magnetic field on the motion of multiphase fluids containing paramagnetic nanoparticles in porous media, in: *SPE Improved Oil Recovery Symposium*, Society of Petroleum Engineers, 2010.